Biophysical Chemistry 196 (2015) 92–99

Contents lists available at ScienceDirect

Biophysical Chemistry

journal homepage: http://www.elsevier.com/locate/biophyschem

Miltefosine and BODIPY-labeled alkylphosphocholine with leishmanicidal activity: Aggregation properties and interaction with model membranes

Marina Berardi Barioni [a], Ana Paula Ramos [b], Maria Elisabete Darbello Zaniquelli [b], Alberto Ulises Acuña [c], Amando Siuiti Ito [a,*]

[a] Departamento de Física, FFCLRP, Universidade de São Paulo, Bandeirantes Avenue 3900, 14040-901 Ribeirão Preto, São Paulo, Brazil
[b] Departamento de Química, FFCLRP, Universidade de São Paulo, Bandeirantes Avenue 3900, 14040-901 Ribeirão Preto, São Paulo, Brazil
[c] Instituto de Química Física "Rocasolano", C.S.I.C., Serrano 119, E-28006 Madrid, Spain

HIGHLIGHTS

- From different methods, miltefosine CMC in aqueous solution was determined as 50 μM.
- Below CMC, miltefosine promotes fluidization of DMPC and DPPC unilamellar vesicles.
- In the critical micelle concentration miltefosine causes loss of vesicles integrity.
- Above CMC, mixed aggregates made of lipids, drug and fluorescent probe are formed.
- The fluorescent analogue MT-EtBDP shows drug pronounced effects in the bilayer core.

GRAPHICAL ABSTRACT

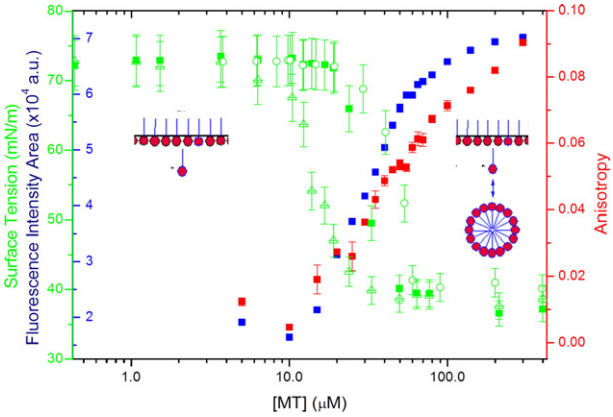

ARTICLE INFO

Article history:
Received 28 August 2014
Received in revised form 8 October 2014
Accepted 8 October 2014
Available online 16 October 2014

Keywords:
Critical micelle concentration (CMC)
BODIPY-alkylphosphocholine
Human leishmaniasis
Leishmanicidal drug

ABSTRACT

Miltefosine (hexadecylphosphocholine, MT) afforded successful oral treatment against human visceral and cutaneous leishmaniasis. Knowledge of MT aggregation in aqueous solutions and of its interaction with lipid membranes is important to understand pharmacokinetics, bioavailability and antiparasitic effects. Methods based on surface tension and fluorescence spectroscopy gave the value of 50 μM for critical micelle concentration (CMC) in buffered water solution, and the value is influenced by salt content. Interaction between MT and lipid vesicles was monitored by fluorescence and the drug promotes only minor changes in the surface of the vesicles. At MT concentration below CMC, modifications in probe fluorescence are due to disordering effects promoted by the drug in the bilayer. Above the CMC, MT promoted large modifications in the vesicles as a whole, resulting in mixed aggregates containing lipids, drug and probe. Effects are less evident above thermal phase transition when the bilayer is in less ordered state.

1. Introduction

Human leishmaniasis is a complex of tropical diseases caused by different species of protozoa parasites of *Leishmania* genus. The disease

* Corresponding author.
E-mail address: amandosi@ffclrp.usp.br (A.S. Ito).

http://dx.doi.org/10.1016/j.bpc.2014.10.002
0301-4622/

is endemic in many countries, mostly located in tropical and subtropical regions, with a worldwide prevalence of 10–12 million, with 1.5 million new cases per year (1,2), and Brazil is the most affected country in American region (3). Clinical manifestations range from self-healing cutaneous lesions to the most severe visceral infection, fatal if left untreated. Current treatment of the disease relies frequently on chemotherapy (4), with organic pentavalent antimonial or pentamidine salts as standard first line option. These drugs require patient hospitalization, show variable clinical response, important secondary effects and are expensive (4,5). An alternative therapy is based on amphotericin B deoxycholate (AmB), an antifungal antibiotic which is nephrotoxic and, therefore, it is best administered as a liposome formulation. In this way AmB is very effective with almost no side effects, but unaffordable in the areas of high prevalence of the disease due to price and storage limitations. The above problems besides that of the ever-increasing resistance against organic antimonials give rise to a major clinical concern fostering the search for alternative treatments of leishmaniasis (5).

Synthetic alkyl ether phospholipids represent a new class of potential antitumor agents that have been shown to induce apoptosis in cancer cells through a mechanism which is only partially understood (6). Some alkylphosphocholines with one or more methylene groups in the alkyl chain replaced by oxygen atoms or carbonyl groups had its activity compared with miltefosine against tumor cells (7). Miltefosine (hexadecylphosphocholine, MT, see Fig. 1A) is a synthetic alkylphosphocholine originally developed for its antineoplastic properties, selectively accumulates in tumor cell membranes (8), but also presents a potent leishmanicidal activity (6,9,10). In recent years, MT afforded the first successful oral treatment against human visceral and cutaneous leishmaniasis, with mild secondary effects (11–14), and it is indicated in India and Germany for that purpose since 2002, and administered as second line treatment for cutaneous leishmaniasis since 2005 in Colombia (15). The successful introduction of MT in the clinical practice contrasts with the incomplete knowledge on its leishmanicidal mechanism at molecular level (16–18). The identification of subcellular MT binding site(s) may yield important clues on the parasiticide mechanism of the drug. In this regard, fluorescent bioactive analogues of MT provide a practical way of determining miltefosine cell distribution and target localization with minimal manipulation and subcellular distortion. In addition, the large absorption coefficients of the fluorescent tags can be very convenient to quantitate the analogue concentration in whole cells or in specific organelles.

The use of fluorescent ligands to assess the affinity and localization of receptors is well documented (19,20), and recent examples show that kinetic and thermodynamic parameters of the drug–receptor interaction can be obtained with emitting analogues, even at a single-cell level (21–24). In the case of lipid compounds, the design of true fluorescent analogues entails preserving as much as possible the amphiphilic properties of the original structure (25,26). Accordingly, miltefosine fluorescent analogues designed for the study of antiparasitic effects were prepared by attaching a non-polar UV-absorbing phenylpolyene fluorescent group to MT alkyl chain, remaining intact the phosphocholine head group which is essential for the in vivo leishmanicidal effect (17,27). These emitting analogues of MT show the same cytotoxicity as the parent drug against amastigote cultures of *L. pifanoi*, and a lower but still potent activity against promastigote cultures of *L. donovani* (17). Fluorescence microscopy images of treated *L. donovani* promastigotes revealed a uniform intracellular distribution of the emitting analogue with a 100-fold enrichment relative to the extracellular concentration, similar to that described for the parent drug MT (17). This was interpreted as due to a common plasma membrane inward translocator for the original drug and its emitting analogues. This large intracellular drug concentration (mM range) would permit substantial binding of MT to low-affinity receptors. All of these observations are consistent with a multi-target leishmanicidal mechanism of MT (17).

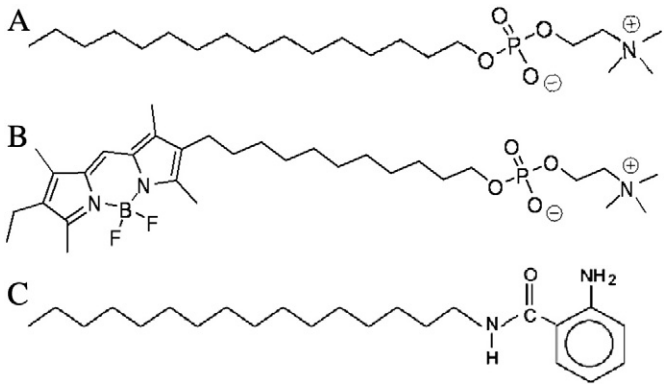

Fig. 1. Chemical structures of the drug miltefosine (MT) (A) and its fluorescent analogue used in this study (6EtBDP-11C-PC or MT-EtBDP) (B) and the fluorescent lipid-probe Ahba (C).

In a second generation of fluorescent MT analogues (28) a substituted lipophilic 4,4-difluoro-4-bora-3a,4a-diaza-*s*-indacene (BODIPY) group was incorporated into terminal positions of the drug alkyl chain (11-(4,4-difluoro-6-ethyl-1,3,5,7-tetramethyl-4-bora-3a,4a-diaza-*s*-indacen-2-il) *n*-undecilphosphatidylcholine, 6Et-BODIPY-11C-PC, hereafter called MT-EtBDP, Fig. 1B). This optical label is much more convenient than the phenylpolyene for biological experiments, since absorption and emission take place in the visible range, with the high brightness and photostability characteristic of BODIPY fluorophore (29,30). The emitting tag was aligned with the polymethylene chain by ligating the substituted BODIPY core at the 2-position. In this way the extended conformation of the original alkyl chain was preserved and the impact of the structural modifications on bioactivity attenuated. The activity of these compounds against promastigote forms of *L. donovani* in vitro was in the μM range, that is, comparable to that of the parent drug. Moreover, the emitting analogues were recognized by the uptake system of *Leishmania*, giving rise to a quick, specific fluorescent staining of the whole living parasite, with the large intracellular enrichment noted above (28).

Considering the amphiphilic properties of the drug, the precise knowledge of MT aggregation in aqueous solutions as well as its interaction with lipid membranes would be of utility to understand MT pharmacokinetics, bioavailability and antiparasitic effects. Notably, previous determinations of MT critical micelle concentration (CMC) values spread over an unacceptable wide range of two orders of magnitude, from 2 μM to 160 μM (31–39). Therefore, in the present work we reinvestigate the CMC of miltefosine in three different media: pure water, 10 mM phosphate buffer solution pH 7.4, and 150 mM NaCl aqueous solution. Two different methods were employed, the first one is based in surface tension properties of MT solutions and the other in emission properties of fluorescent probes. In the first case it used the pendant drop shape analysis technique. The evolution of the drop shape with time allows obtaining dynamic surface tension (DST) curves. Several DST curves were obtained for each studied MT concentration. The values in conditions of diffusion equilibrium, for which the curves reach a plateau, were used for miltefosine CMC determination. Fluorescence spectroscopy was used as a second method to study the aggregation of miltefosine, measuring the change in emission properties of lipophilic fluorescent probes as a function of drug concentration. The probes employed were: 2-amino-N-hexadecylbenzamide (Ahba) (40), which has been shown to monitor micellization processes, and 7-nitrobenz-2-oxa-1,3-diazol-4-yl (NBD) labeled lipids, used as efficient probes to explore the organization and dynamics of molecular assemblies such as membranes, micelles and reverse micelles (41–44).

The interaction of MT with lipid vesicles was studied here using spherical bilayers of zwitterionic phospholipids DMPC (1,2-dimyristoyl-*sn*-glycero-3-phosphocholine) and DPPC (1,2-dipalmitoyl-*sn*-glycero-3-phosphocholine) as simple models of cell membranes. DMPC and

DPPC vesicles were chosen as model membranes because they are well characterized lipid aggregates, whose thermal behavior differs by the phase transition temperature. This allowed us to draw observations in both gel and lipid fluid phases to know how MT affects the bilayer structures in these different phases. A recent work was carried out in vesicles prepared with binary and ternary lipid mixtures, with composition closer to the observed in the parasite membrane (including cholesterol and sphingolipids) and the results should appear in a forthcoming paper. We monitored the steady state and time-resolved fluorescence properties of the lipophilic probes Ahba and NBD-lipids. Furthermore, the emitting analogues of miltefosine described above should present similar amphiphilic properties as the parent drug and might be of utility in the study of pharmacodynamic properties and lipid interactions relevant to miltefosine action mechanism. Therefore, the aggregation properties and CMC of the fluorescent analogue MT-EtBDP were also investigated here, as well as its interaction with model lipid bilayers.

2. Material and methods

2.1. Chemicals

The synthesis of 6Et-BODIPY-11C-PC, or MT-EtBDP, a fluorescent analogue of miltefosine, was carried out as described elsewhere (28). The fluorescent lipophilic probe Ahba (Fig. 1C) was obtained by reaction of hexadecylamine with N-Boc-Abz-COOH using O-benzoil-1-yl-N,N,N′,N′-tetramethyluronium hexafluoroborate (TBTU) and hydroxybenzotriazole (HOBt.H2O), followed by treatment with TFA, as detailed elsewhere (40).

The phospholipids DMPC (1,2-dimyristoyl-sn-glycero-3-phosphocholine) and DPPC (1,2-dipalmitoyl-sn-glycero-3-phosphocholine), and lipid probes 1-palmitoyl-2-[6-(7-nitrobenz-2-oxa-1,3-diazol-4-yl)aminododecanoyl]-sn-glycero-3-phosphocholine (C6-NBD-PC) and (*N*-(7-nitrobenz-2-oxa-1,3-diazol-4-yl)-1,2-dipalmitoyl-sn-glycero-3-phosphoethanolamine) (NBD-PE) from Avanti Polar Lipids (Birmingham, AL, USA). Other reagents as well as miltefosine, used without additional purification, were obtained from Sigma Chemical Co. (St. Louis, MO, USA). Aqueous solutions were prepared using Milli-Q water. The phosphate buffered saline (PBS), at the concentration of 10 mM, was adjusted with NaOH to pH 7.4.

2.2. Vesicle preparation

Large unilamellar lipid vesicles (LUVs) were prepared by extrusion. In brief, a film was formed from a chloroform solution of the corresponding lipid, dried under N_2 and left at reduced pressure for 5 hours, to remove all traces of the organic solvent. The film was first resuspended in phosphate buffer by vortexing to a lipid concentration of 1 mM and then extruded through 0.1 μm pore diameter polycarbonate membranes, maintaining the temperature above the lipid phase transition. In the titration experiments, small aliquots of miltefosine or MT-EtBDP concentrated aqueous stock solutions were added to the sample solution containing the LUVs suspension already prepared with the fluorescent probes.

2.3. Optical absorption and fluorescence measurements

Optical absorption spectra were registered on an Amersham Ultrospec 2100 pro spectrophotometer. A Hitachi F-7000 spectrofluorimeter, with polarizer filters for anisotropy experiments, was used for steady state fluorescence measurements, without any processing for emission spectra correction. Absorption was monitored in order to take into account scattering effects.

Fluorescence lifetimes and time-resolved anisotropy measurements were recorded in a picosecond laser spectrometer, using the time-correlated single-photon counting technique. The excitation source was a mode-locked Ti:Sapphire laser (Tsunami 3950 and Milennia X Spectra Physics) producing 1 ps FWHM pulses with 8.0 MHz pulse repetition rate (3980 Spectra Physics pulse picker). The laser wavelength was selected (GWN-23PL Spectra Physics unit) with second (LBO crystal) and third (BBO crystal) harmonic generators, to yield 460 nm pulses (to excite NBD-lipids) or 330 nm pulses (to excite Ahba and MT-EtBDP), that were directed to an L-format Edinburgh FL900 spectrometer with a monochromator in the emission channel. Single photons were detected by a cooled Hamamatsu R3809U microchannel plate photomultiplier yielding an instrument response function around 100 ps. A Soleil–Babinet compensator in the excitation beam and a Glan–Taylor polarizer in the emission beam were used in anisotropy experiments. Data analysis was carried out by a non-linear least-squares formalism using a commercial package (Edinburgh Instruments). The quality of the fit was evaluated from the reduced-χ^2 values and the residuals distribution.

2.4. Surface tension: pendant drop technique

In aqueous solutions the surface tension at the air–water interface depends on the adsorption of surfactant molecules at that interface. The increase of surfactant bulk concentration causes a decrease in the surface tension, up to the concentration in which the surfactant aggregates in the bulk, forming micelles, and the number of molecules in the interface saturates leading to constant surface tension values. Thus, for CMC determination, several miltefosine aqueous solutions were prepared in the concentration range of 0 to 0.5 mM. Fresh drops were formed in a syringe tip. Measurements were performed using the OCA 20 Tensiometer–Goniometer (Data Physics, Germany). The pendant drops were imaged with a CCD camera over time from the very beginning, after the injection of a concentrated solution of MT to reach the desired concentration of the surfactant in the drop, and the drop profiles were recorded in function of time. The Young–Laplace equation considering the mechanical equilibrium between surface forces and gravity is applied to obtain the surface tension values, by means of DataPhysics SCA software.

3. Results and discussion

3.1. CMC of miltefosine from surface tension measurements

In the pendant drop technique the dynamic surface tension of a drop from a water solution of miltefosine at a given concentration was followed during a time long enough (around 5 minutes) for the drop to attain its mechanical equilibrium provided by the adsorption–desorption and conformational equilibrium. The equilibrium value of surface tension at that specific concentration of MT was then measured to construct a plot of surface tension versus surfactant concentration (see Fig. 2). At the lowest miltefosine concentrations, the surface tension value was not different from that of pure water, ca. 72 mN/m at 25 °C. Increasing MT concentration, the surface tension decreased due to the monomer adsorption in the surface of the drop, until saturation of the surface was attained, when started the formation of micelles in the interior of the drop. From that concentration of MT, the surface tension remained constant and the CMC was graphically determined as the concentration at the intersection of the line corresponding to decrease in the surface tension and the line corresponding to the final state of constant surface tension.

The values obtained for the CMC of MT were 60 ± 5 μM in pure water (Milli-Q water), 50 ± 5 μM in phosphate buffer 10 mM, pH 7.4 and 35 ± 5 μM in the same phosphate buffer with addition of 150 mM NaCl. The differences between the values evidence important electrostatic effects on the micellization process.

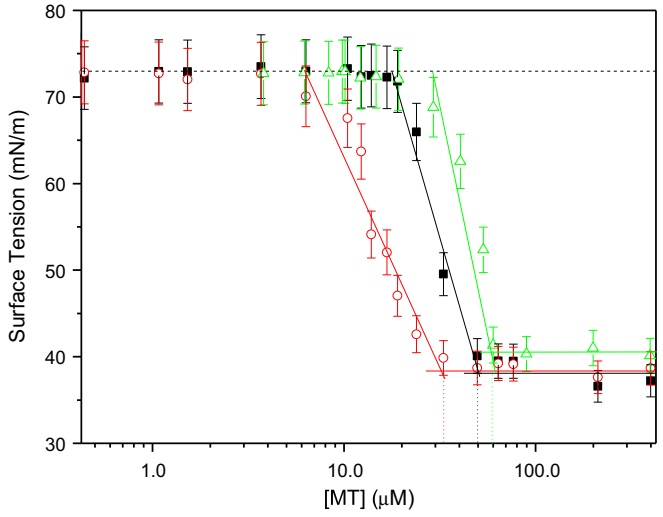

Fig. 2. Miltefosine equilibrium surface tension as a function of MT concentration, as determined by the pendant drop technique, in Milli-Q water (open triangles), PBS 10 mM, pH 7.4 (solid squares) and NaCl 150 mM solution in PBS (open circles) at 25 °C.

3.2. CMC of miltefosine from fluorescence measurements

3.2.1. NBD-lipids

In NBD-PE, the fluorescent NBD label attaches covalently to the head group of a phosphatidylethanolamine molecule. In model membranes, the NBD group has been found to be localized at the membrane–water interface and is uncharged at neutral pH (44). The NBD group of sn-2 acyl chain NBD-labeled phosphatidylcholine (NBD-PC) may loop to a location near the lipid/water interface of phospholipid bilayers and in C6-NBD-PC it does not penetrate the bilayer beyond the C4–C5 atoms of sn-2 chains of the host lipid (45). The probes are able to monitor structural changes in lipid bilayers like those occurring in thermal phase transition of lipid vesicles (46,47).

At the small concentration of NBD-lipids employed in the work (1 μM), the florescence emission in buffer solution was very low. With the addition of aliquots of miltefosine, the intensity of emission gradually increased, due to interaction of NBD-lipids with monomers and aggregates of miltefosine. A plateau is reached above 100 μM of the drug and the changes in intensity as function of concentration are related to MT micellization process. The value of the CMC of miltefosine was obtained from the intersection of the curves describing the initial phase of insertion of the probe in the pre-micelle aggregates and the final phase where all the probes are inserted in the miltefosine micelles. A similar behavior was observed in anisotropy measurements: initial increase with the addition of miltefosine and stabilization at high concentration of surfactant (above 100 μM). From the experimental plots of intensity and anisotropy of C6-NBD-PC and NBD-PE as a function of MT concentration (see Fig. 3) we determined the CMC in buffer as equal to 50 ± 10 μM. The values in water are slightly higher, reaching 60 ± 10 μM and in the presence of salt the value fluctuated from 25 to 60 μM.

3.2.2. Amino-hexadecylbenzamide probe

The hydrophobic probe Ahba forms aggregates in water solution, characterized by a very weak red-shifted fluorescence emission (40,48). Interaction with surfactant molecules disrupts the aggregates, and above micellization of the surfactant, probe molecules partition preferentially into the micelles, giving rise to a large increase in fluorescence intensity and a blue shift of the emission spectrum. In this way, the micellization processes of well characterized surfactant compounds have been followed in great detail, as e.g. sodium dodecyl sulfate (SDS), cetyl trimethylammonium bromide (CTAB) and dimethyl dodecylammonium propane sulfonate (DPS) (40).

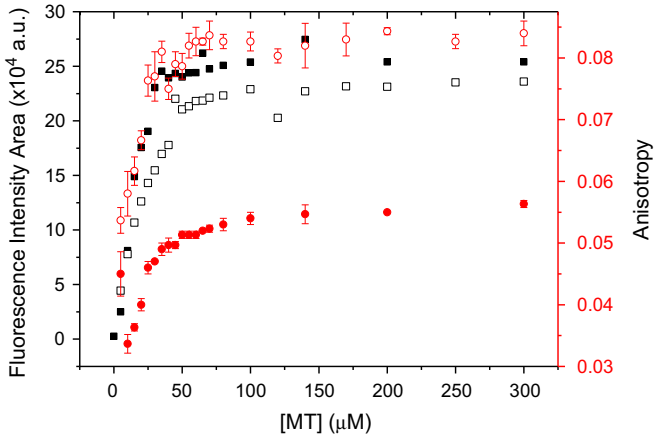

Fig. 3. Variation of fluorescence intensity calculated as the area under the emission spectra (squares) and fluorescence anisotropy (circles) of the probes NBD-PE (solid) and C6-NBD-PC (open) in PBS 10 mM, pH 7.4 with the addition of MT. λ_{exc} = 460 nm, T = 25 °C.

In the experiments with MT, we observed an initial steep rise in the Ahba fluorescence intensity with the addition of the drug (see Fig. 4), and a plateau in intensity, stabilized at high concentrations of MT. We determined the CMC of miltefosine from the intercept of the two straight lines representing the two phases of intensity variation. The fluorescence anisotropy of Ahba also depends on its interaction with MT. In the absence of MT the fluorescence polarization is very low, possibly due to exciton interactions and energy homotransfer among probe molecules within the aggregates. The addition of MT decreases homotransfer increasing the emission anisotropy, which rises until the CMC is attained. From Ahba fluorescence, the CMC of miltefosine was determined as 50 ± 10 μM in phosphate buffer 10 mM, pH 7.4, and in Milli-Q water. With the addition of 150 mM NaCl the CMC decreased to 25 ± 10 μM (Table 1).

As noted above, published values of CMC of miltefosine in aqueous solutions extend over a wide range, from 2.0 to 160 μM. The lowest values were obtained from surface tension measurements in Langmuir trough monolayers (35,36), while slightly higher values, around 10 μM, were determined using surface tension techniques based on the Du Nouy ring (35–37) or Wilhelmy plates (31,32). Using a spectroscopic technique based on fluorescence changes of a pyrene probe McDonald et al. (34) found a value of 32 μM (water, 20 °C) The same technique in the hands of Kang et al. (33) yielded a much higher value, ca. 160 μM, although in this last case the corresponding titration plots appear incomplete. In some of the experiments listed above (e.g. (31,36)), miltefosine CMC

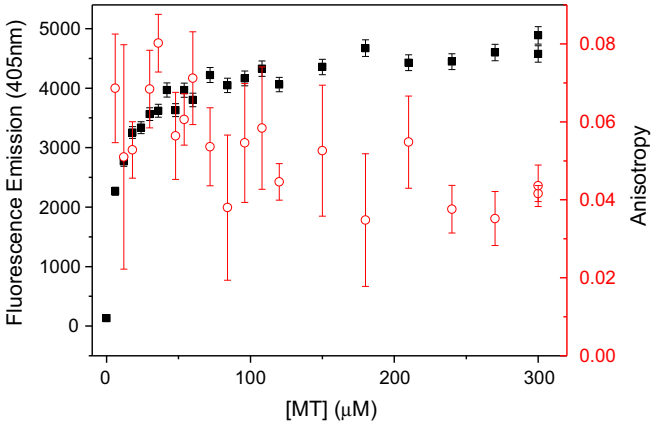

Fig. 4. Fluorescence intensity (solid squares) and steady-state anisotropy (open circles) of Ahba aqueous (Milli-Q water) suspensions (20 μM) as a function of MT concentration. λ_{exc} = 310 nm, T = 25 °C.

Table 1
Miltefosine critical micelle concentration (CMC, μM) determined using different methods, in Milli-Q water, PBS 10 mM, pH 7.4 and PBS with addition of 150 mM NaCl.

	Milli-Q water	PBS 10 mM pH 7.4	PBS + 150 mM NaCl
Surface tension	60 ± 5	50 ± 5	35 ± 5
Florescence Ahba	60 ± 10	50 ± 10	25 ± 10
Fluorescence C6-NBD-PC	60 ± 10	50 ± 10	50 ± 20
Fluorescence NBD-PE	65 ± 10	45 ± 10	60 ± 20
Fluorescence MT-EtBDP	–	50 ± 10	–

was independent of NaCl concentration, even for salt concentrations as high as 250 mM.

The miltefosine CMC values reported here in aqueous solution at 25 °C are consistent, since there is good agreement between the values measured by two quite different techniques. It is also shown here that CMC of miltefosine is influenced by salt contents. Phosphocholine lipids in water solution are zwitterionic and remain isoelectric in a wide pH range (3–13 pH units for egg lecytine (49)). Thus, electrostatic effects on the micelle-forming process may be in the source of the discrepant previous CMC values noted above. In fact, important electrostatic effects have been found in the study of the concentration of halide ions at the interface of zwitterionic micelles of zwitterionic amphiphilic 3-(N-hexadecyl-N, N-dimethylammonio) propane sulfonate (HPS) and miltefosine itself (50). In our experiments, despite the larger fluctuations observed in the values measured in the presence of NaCl, the values of the CMC of miltefosine remained around 50 μM and decreased in the order Milli-Q > buffer > buffer with NaCl (Table 1).

3.2.3. The fluorescent miltefosine analogue MT-EtBDP

The fluorescent analogue MT-EtBDP is an amphiphilic lipid-like compound that aggregates in water solution, most likely forming micelles as the parent drug. In ethanol solution, the shape of the absorption spectrum is independent of MT-EtBDP concentration (28), with a maximum peak at 529 nm and a shoulder in 502 nm (see Fig. 5). However, in aqueous solutions, the shape of the spectrum is strongly dependent on the analogue concentration and a large increase in the intensity of the shoulder at 502 nm, compared to the peak in 529 nm, was observed at increasing analogue concentration (Fig. 5). This likely results from excitonic interactions among BODIPY groups within MT-EtBDP aggregates (51) which apparently already takes place at concentrations as low as 10 μM. The observation indicates that even at the lowest concentration the large hydrophobicity of the labeled drug gives rise to a heterogeneous population of aggregates.

Fluorescence spectra and anisotropy values of aqueous solutions of MT-EtBDP were used to obtain the CMC of miltefosine. Fluorescence data of MT-EtBDP presented the same pattern of changes observed with Ahba and NBD-lipids, with the addition of the drug (Fig. 6). The value of 50 μM was obtained for the CMC of MT in phosphate buffer, in agreement with the results presented before using the other probes.

3.3. MT interaction with DMPC and DPPC lipid vesicles

3.3.1. Fluorescence of the probe Ahba

The fluorescent lipid probe Ahba was used at Ahba/phospholipid ratio of 2 mol%. It was previously observed that at this concentration the probe has maximum emission at 404 nm and inserts into the lipid bilayer, with the aminophenyl group close to the lipid polar-head region (40). The addition of MT did not modify substantially the absorption and emission spectra of Ahba, apart from a small (about 10%) increase in emission intensity, similar to the increase of its single-exponential lifetime, from 8.3 ns to 8.5 ns (52). The steady state fluorescence anisotropy of Ahba in LUVs made up from pure phospholipid was comparable with that reported previously (40), 0.048 in DMPC and 0.034 in DPPC, and the addition of MT (until 5 mol% drug/lipid molar ratio) did not change significantly those values. Moreover, the time-resolved anisotropy decay of Ahba in LUVs of DMPC and DPPC containing a MT/phospholipid ratio of 5 mol% was the same as that measured in the pure phospholipid (52). Thus, the dynamics of the polar region of the phospholipid bilayer remained largely unaffected with the addition of MT to DMPC or DPPC vesicles up to 5 mol% drug/lipid ratio.

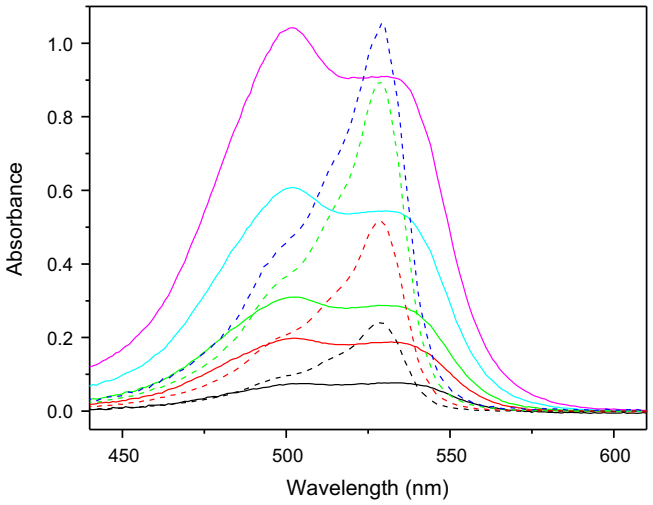

Fig. 5. Absorption spectra of MT-EtBDP increasing with MT addition from 10, 30, 50 up to 60 μM in ethanol (dashed lines) and from 10, 30, 50, 100 up to 160 μM in PBS 10 mM, pH 7.4 (solid lines), at 25 °C.

3.3.2. Fluorescence of the probes NBD-lipids

We followed the fluorescence of NBD-lipid probes inserted in DMPC and DPPC LUVs (at ratio of 1 mol%), under the addition of miltefosine. The experiments were performed in temperatures below and above the temperature of the main phase transition temperature T_m of the lipid bilayers (23 °C for DMPC and 41 °C for DPPC). The head group labeled NBD-PE is in the polar region of the bilayer (41). In vesicles of DPPC in the fluid phase, the NBD group in the probe C6-NBD-PC is located in the region of the glycerol backbone and it loops to a transverse location closer to the interface (53). Below the phase transition T_m, the NBD group in NBD-PC may localize in deeper regions of the bilayer, with a distribution along the membrane axis (47).

In the absence of miltefosine the intensity decay profiles of the NBD-lipids in DMPC and DPPC vesicles were fitted to bi-exponential curves, dominated by a long lifetime component that presented pre-exponential factor above 0.60 (Table 2). The long lifetime values at 15 °C were near to 10 ns, which decreased to values between 6.0 and 8.0 ns for the vesicles in the lipid fluid phase. Short lifetime component

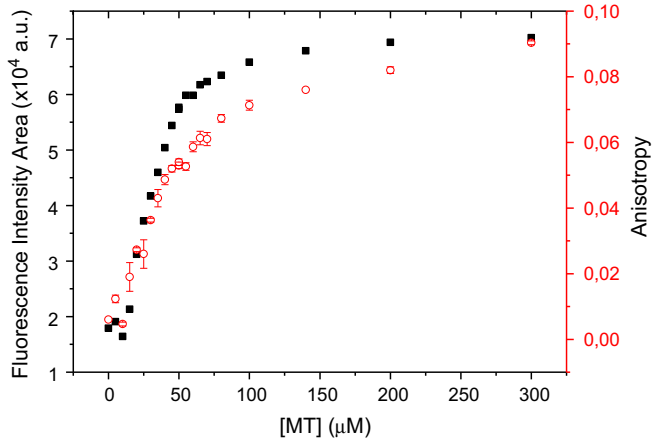

Fig. 6. Variation of fluorescence intensity calculated as the area under the emission spectra (solid squares) and fluorescence anisotropy (open circles) of the fluorescent analogue MT-EtBDP in PBS 10 mM, pH 7.4 with addition of MT. λ_{exc} = 530 nm, T = 25 °C.

(between 2.0 and 4.0 ns, Table 2) contribute less to the decay, with pre-exponential factor below 0.4. The decay was fastened at temperatures above the thermal phase transition, as can be seen by the decrease in the average lifetimes (Table 2). In agreement with previous reports (47), the fluorescence lifetimes of NBD-PE were more affected by thermal changes in DPPC vesicles than those of C6-NBD-PC and we observed similar behavior in DMPC vesicles.

Although lifetimes by themselves did not afford a clear distinction of different regimes in the modifications of the bilayers (Fig. 7A), the pre-exponential factor clearly reveals the change in distribution of the probes between two populations in the vesicles that occurs when MT was added in concentrations above the CMC (Fig. 7B). As the average lifetime calculation incorporates contributions from both lifetime and pre-exponential factor, that parameter gives a better description of the effects promoted by MT on DMPC and DPPC vesicles (Fig. 8). The rate of decrease in average lifetimes (seen by the inclination of the plot in Fig. 8) due to the incorporation of MT in the bilayers is higher at the initial steps of the titration and suffers a sudden decrease at MT concentrations near the CMC in buffer solution. Thus, the time-resolved data indicates that the addition of the drug gradually affects the environment around the fluorescent probe, and the increased disorder promoted by MT, decrease both the long and short lifetime. At the CMC, MT can affect the bilayer in larger extent, reflected in the change in the distribution of the populations of the probe in the bilayer. However, above the CMC the changes in the environment around the probe are less affected by the addition of MT, with minor influence in the deexcitation processes of the fluorescent probe. It is noticeable that the changes are more pronounced when the lipids in the vesicle are in the gel phase (low temperatures) than when they are in the lipid fluid phase (high temperatures). This could be expected since the bilayer structure above the lipid phase transition is already in a less ordered state reducing the overall disordering effect promoted by MT.

The anisotropy values are affected by relatively larger experimental errors compared to the lifetime measurements. However we can discern also here the occurrence of two regimes in the modifications imposed by MT on the bilayers: when MT is below the CMC the anisotropy of the probe in the gel phase remains relatively insensitive to the addition of the surfactant at low temperature and slightly decreases at high temperature. Above CMC, unexpected increase in anisotropy was observed (see Fig. 9). As the drug in the higher concentration is acting as aggregates, the anisotropy of the probe may be reflecting not the rotational diffusion of the probe in the bilayer, but a more complex behavior of larger aggregates containing the drug, the probe and the lipids. In higher temperatures the bilayer is in the lipid fluid phase and

Table 2
Intensity decay parameters (lifetime τ_i, normalized pre-exponential factor α_i and average lifetime τ_{ave}) obtained from time-resolved intensity profiles measured for NBD-lipids (5 μM) in DMPC and DPPC 1 mM vesicles, in PBS, pH 7.4 at MT concentration 0 and 100 μM, at gel (15 °C) and fluid (35 °C for DMPC and 55 °C for DPPC vesicles) lipid phases. λ_{exc} = 465 nm, λ_{em} = 530 nm. Relative errors for fitted parameters are below 2%.

Lipid	Probe	T	[MT] (μM)	τ_1 (ns)	α_1	τ_2 (ns)	α_2	τ_{ave} (ns)
DMPC	NBD-PE	15 °C	0	11.6	0.74	3.7	0.26	10.8
			100	10.4	0.65	3.7	0.35	9.3
		35 °C	0	8.5	0.81	2.1	0.19	8.2
			100	8.0	0.81	1.6	0.19	7.7
	C6-NBD-PC	15 °C	0	10.2	0.71	1.8	0.29	8.2
			100	8.4	0.63	2.0	0.37	7.7
		35 °C	0	7.8	0.99	0.1	0.01	7.8
			100	7.4	0.82	0.8	0.18	7.3
DPPC	NBD-PE	15 °C	0	11.6	0.59	3.8	0.41	10.2
			100	11.6	0.51	4.2	0.49	9.7
		55 °C	0	6.2	0.81	1.8	0.19	5.7
			100	6.1	0.81	1.8	0.19	5.8
	C6-NBD-PC	15 °C	0	9.3	0.61	2.8	0.39	8.2
			100	8.1	0.59	3.0	0.41	7.1
		55 °C	0	6.4	0.80	3.1	0.20	6.0
			100	5.7	0.86	1.9	0.14	5.5

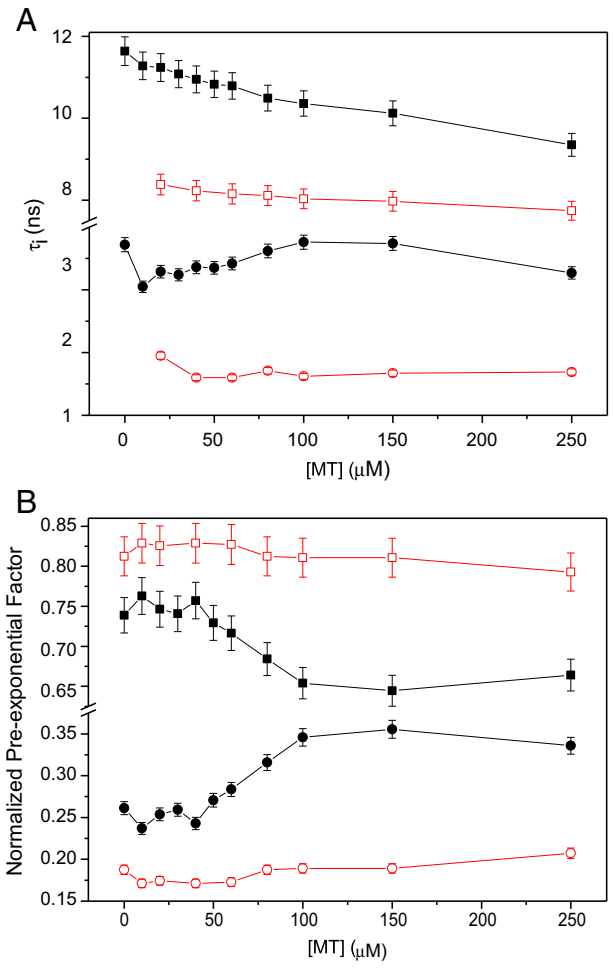

Fig. 7. Lifetimes, τ_i (A) and pre-exponential factors, α_i (B) obtained from bi-exponential fit (τ_1, α_1 squares and τ_2, α_2 circles) of intensity decay profiles of the probe NBD-PE 1 mol% in LUVs of DMPC 1 mM measured at 15 °C (solid) and 35 °C (open). λ_{exc} = 460 nm, λ_{em} = 530 nm.

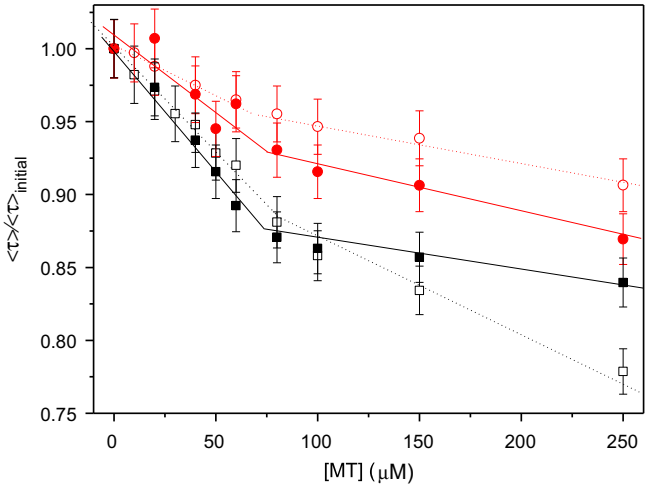

Fig. 8. Effect of MT on decay of NBD-PE (5 μM) in DMPC 1 mM LUVs (1 mM) (open symbols, dotted lines) and of C6-NBD-PC in DPPC 1 mM LUVs (solid symbols, solid lines). Plots, as a function of MT concentration, of the ratio between average lifetime with addition of MT and initial value without MT. Temperatures below (15 °C) (squares) and above the lipid phase transition (35 °C for DMPC and 55 °C for DPPC) (circles).

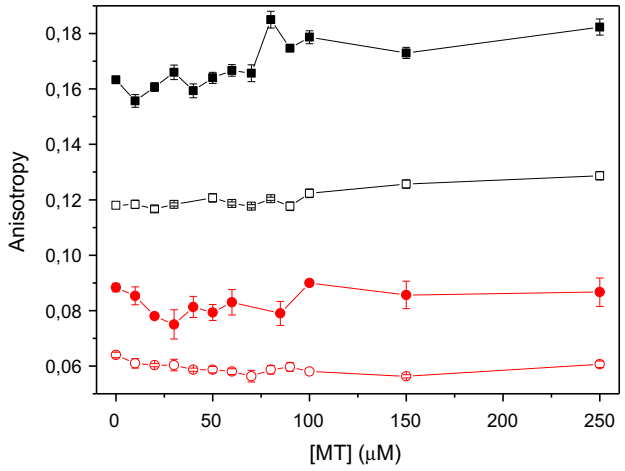

Fig. 9. Anisotropy of NBD-PE (1 mol%) in DMPC 1 mM LUVs (open) and of C6-NBD-PC (1 mol%) in DPPC 1 mM LUVs (solid) below (15 °C) (squares) and above the lipid phase transition (35 °C for DMPC and 55 °C for DPPC) (circles), as a function of MT concentration.

in the initial steps of surfactant addition, the decrease in anisotropy of the probe reflects the increased lipid disorder. It is observed that at MT concentrations above the CMC the anisotropy follows a trend similar to that observed at lower temperature, noticing however that the values of anisotropy in DMPC vesicles at 35 °C are considerably lower than at 15 °C. Similar behavior was observed for the NBD-PE probe in DPPC vesicles, as well as for C6-NBD-PC in both LUVs.

In this way, taking the results as a whole, it is proposed that the addition of MT in concentrations below the CMC causes a disordering effect in the bilayer of DMPC or DPPC vesicles. Above the CMC, drastic changes occur, causing formation of aggregates of the lipids and miltefosine, with disruption of the bilayer.

3.3.3. MT-EtBDP interaction with phospholipid vesicles

MT-EtBDP was added in amounts corresponding to bulk concentration between 0 and 50 μM to LUVs made up from DMPC or DPP28C, that is, in MT/phospholipid ratio from 0 to 5 mol%. The absorption spectrum of the labeled drug presented a maximum at 533 nm, slightly red shifted from the value reported in ethanol solution (28) or in aqueous solutions and the peak of emission displaced from 530 nm in water to values above 540 nm in the presence of DMPC or DPPC vesicles. At low concentrations (below 10 μM), intensity decay profiles of MT-EtBDP added to the vesicles were fitted to a monoexponential curve with lifetime around 7.0 ns (Table 3). Increasing the concentration, the decay becomes complex and three exponentials fit the experimental curves: short lifetimes, around 1.0 ns, dominated the decay, and a small contribution of a long lifetime, above 10 ns, was necessary to fit the data (Table 3). The average lifetimes continuously decreased with increase in MT-EtBDP concentration in the vesicles.

The time-resolved anisotropy decay profiles were best fitted to monoexponential curves (Table 3). The rotational correlation time, θ, gradually decreased with rising concentration of MT-EtBDP, showing that the diffusional rotation increases due to reduction of the microviscosity of the bilayer, a result of the disordering effect promoted by the molecule. At higher concentrations, the compound may form microregions in the bilayer, leading to the observed decrease in the initial anisotropy due to energy homotransfer.

4. Conclusions

The critical micelle concentration (CMC) of miltefosine was determined using three different methods: (i) measurements of surface tension of a drop of aqueous solution of MT, (ii) measurements of fluorescence intensity and (iii) anisotropy of the lipophilic probe Ahba and of NBD labeled lipids. The results presented good agreement, and at 25 °C the CMC of MT was 60 ± 10 μM in pure Milli-Q water, and 50 ± 10 μM in phosphate buffer 10 mM (pH 7.4). Some discrepancy arose in measurements in phophate buffer containing 150 mM NaCl and a value of 40 ± 20 μM was obtained as a mean result from the different methods. In general terms, in our experiments, the CMC of miltefosine was dependent of the presence of ions in the medium and decreased in the order Milli-Q > buffer > buffer with NaCl (Table 1).

Optical absorption spectra of the fluorescent analogue MT-EtBDP in aqueous medium, compared to those in ethanol, show that the hydrophobicity of the labeled drug originates an heterogeneous population of aggregates. From flourescence spectroscopy parameters of BODIPY in the analogue, the value of CMC of MT-EtBDP was determined as 50 μM in phosphate buffer.

Effects due to the addition of aliquots of MT to DMPC or DPPC vesicles were monitored by the fluorescence emission of the lipophilic probe Ahba inserted in the vesicles at 2 mol% concentration. Fluorescence parameters of Ahba slightly changed with the addition of MT, until MT/phospholipids ratios of 5 mol%. As the fluorescent group of the probe is located in the polar head region of the bilayers, the results show that MT promotes small change in that region of the vesicles.

Changes in DMPC and DPPC vesicles upon the addition of MT were examined also by monitoring the fluorescence of NBD-lipids. Despite different locations in the bilayer, both NBD-PE and C6-NBD-PC inserted in DMPC or DPPC vesicles displayed similar features upon the addition of miltefosine. Drastic changes were observed in the distribution of long and short lifetime populations determined from intensity decay profiles when miltefosine concentration was above the CMC. The changes in average lifetimes as well as in the steady state anisotropy of NBD-PE or C6-NBD-PC gave the following picture for the effects promoted by MT in the bilayers: when the concentration of MT is below the CMC, the modifications in NBD-lipid fluorescence are largely due to disordering effects in the bilayer, promoted by the drug; in concentrations above the CMC the NBD fluorescence parameters were less sensitive to the addition of MT. The drug, acting as an aggregate, does not modify the local environment around the fluorescent moiety, but promotes large changes in the bilayer that may loose integrity and behaves

Table 3
Intensity decay parameters (lifetime τ_i, normalized pre-exponential factor α_i and average lifetime τ_{ave}) obtained from time-resolved intensity profiles and initial anisotropy r_0 and rotational correlation times θ obtained from fitting of anisotropy decay profiles measured for MT-EtBDP in LUVs made up from DPPC, as a function of probe/lipid ratio P:L in mol%. Lipid concentration of 1 mM in phosphate buffer 10 mM, pH 7.4. λ_{exc} = 505 nm, λ_{em} = 537 nm, T = 50 °C. Relative errors for fitted parameters are below 2%. Relative errors for calculated average lifetime are 5%.

[MT-EtBDP] (μM)	P:L	τ_1 (ns)	α_1	τ_2 (ns)	α_2	τ_3 (ns)	α_3	τ_{ave} (ns)	r_0	θ (ns)
1	0.1	–	–	7.0	1	–	–	7.0	0.21	1.95
2.5	0.25	–	–	6.9	1	–	–	6.9	0.25	1.73
10	1	0.82	0.08	6.0	0.92	–	–	5.9	0.20	1.05
20	2	0.84	0.16	4.0	0.78	9.8	0.06	4.8	0.14	0.83
30	3	1.6	0.54	3.6	0.44	18	0.02	4.8	0.16	0.67
40	4	1.2	0.71	2.9	0.25	12	0.04	4.3	0.09	0.78
50	5	0.94	0.77	2.6	0.18	12	0.05	5.1	0.09	0.93

then as mixed aggregates containing lipids, drug and probe. Effects are more evident at low temperature since above the thermal phase transition the bilayer is already in a less ordered state and changes promoted by the drug are relatively smaller compared to those observed when the bilayer is in the gel phase.

The BODIPY group in MT-EtBDP allowed a direct observation of changes promoted by the compounds in lipid vesicles. Changes in spectral position, intensity and steady state anisotropy, complemented by fluorescence and anisotropy decay profiles, showed that MT-EtBDP gradually decreased the order and increased the fluidity of the bilayer. The location of the fluorophore in the tail of the aliphatic chain demonstrated that MT has pronounced effects in the interior of the vesicle bilayer, without great modifications in the polar head region, as verified with the probe Ahba.

Acknowledgments

The authors thank FAPESP (Processo 09/54044-3) and CNPq (Processo: 304981/2012-5) for financial support. This work was supported by projects EU QlK2-CT-2001-01404, RD06/ 0021/0006 and PI061125 (from Fondo de Investigaciones Sanitarias, FIS, Ministerio de Sanidad y Consumo of Spain) and CTQ2010-16457 (from Ministerio de Ciencia e Innovacion, Spain). MBB acknowledges a fellowship from FAPESP 2010/08652-9, ASI is member of INCT-FCx Brazil.

References

[1] P. Desjeux, Leishmaniasis: current situation and new perspectives, Comp. Immunol. Microbiol. Infect. Dis. 27 (5) (2004) 305–318.
[2] H.W. Murray, et al., Advances in leishmaniasis, Lancet 366 (9496) (2005) 1561–1577.
[3] J. Alvar, et al., Leishmaniasis worldwide and global estimates of its incidence, PLoS ONE 7 (5) (2012).
[4] J. Alvar, S. Croft, P. Olliaro, Chemotherapy in the treatment and control of leishmaniasis, Adv. Parasitol. 61 (2006) 223–274.
[5] S.L. Croft, S. Sundar, A.H. Fairlamb, Drug resistance in leishmaniasis, Clin. Microbiol. Rev. 19 (1) (2006) 111–126.
[6] C. Gajate, F. Mollinedo, Biological activities, mechanisms of action and biomedical prospect of the antitumor ether phospholipid ET-18-OCH3 (edelfosine), a proapoptotic agent in tumor cells, Curr. Drug Metab. 3 (5) (2002) 491–525.
[7] M. Agresta, et al., Synthesis and antiproliferative activity of alkylphosphocholines, Chem. Phys. Lipids 126 (2) (2003) 201–210.
[8] B.M. Castro, et al., Edelfosine and miltefosine effects on lipid raft properties: membrane biophysics in cell death by antitumor lipids, J. Phys. Chem. B 117 (26) (2013) 7929–7940.
[9] A. Kuhlencord, et al., Hexadecylphosphocholine — oral treatment of visceral leishmaniasis in mice, Antimicrob. Agents Chemother. 36 (8) (1992) 1630–1634.
[10] S.L. Croft, M.P. Barrett, J.A. Urbina, Chemotherapy of trypanosomiases and leishmaniasis, Trends Parasitol. 21 (11) (2005) 508–512.
[11] H. Sindermann, J. Engel, Development of miltefosine as an oral treatment for leishmaniasis, Trans. R. Soc. Trop. Med. Hyg. 100 (2006) S17–S20.
[12] J. Soto, P. Soto, Miltefosine: oral treatment of leishmaniasis, Expert Rev. Anti-Infect. Ther. 4 (2) (2006) 177–185.
[13] S. Sundar, M. Rai, Treatment of visceral leishmaniasis, Expert. Opin. Pharmacother. 6 (16) (2005) 2821–2829.
[14] S.L. Croft, et al., The activity of alkyl phosphorylcholines and related derivatives against leishmania-donovani, Biochem. Pharmacol. 36 (16) (1987) 2633–2636.
[15] O.L. Fernandez, et al., Miltefosine and antimonial drug susceptibility of *Leishmania Viannia* species and populations in regions of high transmission in Colombia, PLoS Negl. Trop. Dis. 8 (5) (2014).
[16] S.L. Croft, K. Seifert, M. Duchene, Antiprotozoal activities of phospholipid analogues, Mol. Biochem. Parasitol. 126 (2) (2003) 165–172.
[17] J.M. Saugar, et al., Synthesis and biological evaluation of fluorescent leishmanicidal analogues of hexadecylphosphocholine (miltefosine) as probes of antiparasite mechanisms, J. Med. Chem. 50 (24) (2007) 5994–6003.
[18] G. Barratt, M. Saint-Pierre-Chazalet, P.M. Loiseau, Cellular Transport and Lipid Interactions of Miltefosine, Curr. Drug Metab. 10 (3) (2009) 247–255.
[19] J.C. McGrath, S. Arribas, C.J. Daly, Fluorescent ligands for the study of receptors, Trends Pharmacol. Sci. 17 (11) (1996) 393–399.
[20] J.C. McGrath, C.J. Daly, Do fluorescent drugs show you more than you wanted to know? Br. J. Pharmacol. 139 (2) (2003) 187–189.
[21] A.A. Souto, et al., New fluorescent water-soluble taxol derivatives, Angew. Chem. Int. Ed. 34 (23–24) (1995) 2710–2712.
[22] C. Gajate, et al., Intracellular triggering of fas aggregation and recruitment of apoptotic molecules into fas-enriched rafts in selective tumor cell apoptosis, J. Exp. Med. 200 (3) (2004) 353–365.
[23] M. Abal, et al., Centrosome and spindle pole microtubules are main targets of a fluorescent taxoid inducing cell death, Cell Motil. Cytoskeleton 49 (1) (2001) 1–15.
[24] M.P. Lillo, et al., Location and properties of the taxol binding center in microtubules: A picosecond laser study with fluorescent taxoids, Biochemistry 41 (41) (2002) 12436–12449.
[25] C.R. Mateo, et al., New fluorescent octadecapentaenoic acids as probes of lipid membranes and protein-lipid interactions, Biophys. J. 71 (4) (1996) 2177–2191.
[26] E. Quesada, A.U. Acuna, F. Amat-Guerri, New transmembrane polyene bolaamphiphiles as fluorescent probes in lipid bilayers, Angew. Chem. Int. Ed. 40 (11) (2001) 2095–2097.
[27] E. Quesada, et al., Synthesis and spectral properties of Amphiphilic lipids with linear conjugated polyene and phenylpolyene fluorescent groups, Eur. J. Org. Chem. 14 (14) (2007) 2285–2295.
[28] V. Hornillos, et al., Synthesis of BODIPY-labeled alkylphosphocholines with leishmanicidal activity, as fluorescent analogues of miltefosine, Bioorg. Med. Chem. Lett. 18 (24) (2008) 6336–6339.
[29] A. Loudet, K. Burgess, BODIPY dyes and their derivatives: Syntheses and spectroscopic properties, Chem. Rev. 107 (11) (2007) 4891–4932.
[30] G. Ulrich, R. Ziessel, A. Harriman, The chemistry of fluorescent bodipy dyes: Versatility unsurpassed, Angew. Chem. Int. Ed. 47 (7) (2008) 1184–1201.
[31] P.S. de Araujo, et al., Structure and Thermodynamic Properties of the Complexes between Phospholipase a2 and Lipid Micelles, Biochemistry 18 (4) (1979) 580–586.
[32] B. de Castro, et al., Interaction of drugs with hexadecylphosphocholine micelles. Derivative spectroscopy, acid-base and solubility studies, Mater. Sci. Eng. C Biomim. Supramol. Syst. 18 (1-2) (2001) 71–78.
[33] E.C. Kang, S. Kataoka, K. Kato, Synthesis and properties of alkyl phosphorylcholine amphiphiles with a linear and an asymmetrically branched alkyl chain, Bull. Chem. Soc. Jpn. 78 (8) (2005) 1558–1564.
[34] P.M. Macdonald, et al., Synthesis and Characterization of a Homologous Series of Zwitterionic Surfactants Based on Phosphocholine, Langmuir 7 (11) (1991) 2602–2606.
[35] M. Rakotomanga, P.M. Loiseau, M. Saint-Pierre-Chazalet, Hexadecylphosphocholine interaction with lipid monolayers, Biochim. Biophys. Acta Biomembr. 1661 (2) (2004) 212–218.
[36] M. Rakotomanga, M. Saint-Pierre-Chazalet, P.M. Loiseau, Alteration of fatty acid and sterol metabolism in miltefosine-resistant *Leishmania donovani* promastigotes and consequences for drug-membrane interactions, Antimicrob. Agents Chemother. 49 (7) (2005) 2677–2686.
[37] A. Yaseen, et al., Adsorption of single chain zwitterionic phosphocholine surfactants: effects of length of alkyl chain and head group linker, Biophys. Chem. 117 (3) (2005) 263–273.
[38] A. Yaseen, et al., Surface adsorption of zwitterionic surfactants: n-alkyl phosphocholines characterised by surface tensiometry and neutron reflection, J. Colloid Interface Sci. 288 (2) (2005) 361–370.
[39] M. Yaseen, et al., The structure of zwitterionic phosphocholine surfactant monolayers, Langmuir 22 (13) (2006) 5825–5832.
[40] C.A. Marquezin, et al., Spectroscopic characterization of 2-amino-N-hexadecylbenzamide (AHBA), a new fluorescence probe for membranes, Biophys. Chem. 124 (2) (2006) 125–133.
[41] A. Chattopadhyay, Chemistry and biology of N-(7-Nitrobenz-2-oxa-1,3-diazol-4-Yl)-labeled lipids — fluorescent-probes of biological and model membranes, Chem. Phys. Lipids 53 (1) (1990) 1–15.
[42] D.A. Kelkar, A. Chattopadhyay, Depth-dependent solvent relaxation in reverse micelles: a fluorescence approach, J. Phys. Chem. B 108 (32) (2004) 12151–12158.
[43] H. Raghuraman, S.K. Pradhan, A. Chattopadhyay, Effect of urea on the organization and dynamics of triton X-100 micelles: a fluorescence approach, J. Phys. Chem. B 108 (7) (2004) 2489–2496.
[44] S. Mukherjee, et al., Organization and dynamics of N-(7-nitrobenz-2-oxa-1,3-diazol-4-yl)-labeled lipids: a fluorescence approach, Chem. Phys. Lipids 127 (1) (2004) 91–101.
[45] L.M.S. Loura, et al., Effects of fluorescent probe NBD-PC on the structure, dynamics and phase transition of DPPC. A molecular dynamics and differential scanning calorimetry study, Biochim. Biophys. Acta Biomembr. 1778 (2) (2008) 491–501.
[46] J.M.I. Alakoskela, P.K.J. Kinnunen, Probing phospholipid main phase transition by fluorescence spectroscopy and a surface redox reaction, J. Phys. Chem. B 105 (45) (2001) 11294–11301.
[47] H. Raghuraman, S. Shrivastava, A. Chattopadhyay, Monitoring the looping up of acyl chain labeled NBD lipids in membranes as a function of membrane phase state, Biochim. Biophys. Acta Biomembr. 1768 (5) (2007) 1258–1267.
[48] M. Takara, et al., Solvent effects in optical spectra of ortho-aminobenzoic acid derivatives, J. Fluoresc. 19 (6) (2009) 1053–1060.
[49] A.D. Bangham, R.M.C. Dawson, Relation between the activity of a lecithinase and the electrophoretic charge of the substrate, Biochem. J. 72 (1959) 486–492.
[50] I.M. Cuccovia, L.S. Romsted, H. Chaimovich, Determination of halide concentrations at the interface of zwitterionic micelles by chemical trapping: influence of the orientation of the dipole and the nature of the cation, J. Colloid Interface Sci. 220 (1) (1999) 96–102.
[51] F. Bergstrom, et al., Dimers of dipyrromethene boron difluoride (BODIPY) with light spectroscopic applications in chemistry and biology, J. Am. Chem. Soc. 124 (2) (2002) 196–204.
[52] L. Alonso, et al., Interaction of miltefosine with intercellular membranes of stratum corneum and biomimetic lipid vesicles, Int. J. Pharm. 434 (1–2) (2012) 391–398.
[53] L.M.S. Loura, J.P.P. Ramalho, Location and dynamics of acyl chain NBD-labeled phosphatidylcholine (NBD-PQ in DPPC bilayers A molecular dynamics and time-resolved fluorescence anisotropy study, Biochim. Biophys. Acta Biomembr. 1768 (3) (2007) 467–478.